Charged particle multiplicity distributions in restricted rapidity intervals in Z^0 hadronic decays[*]

DELPHI Collaboration

P. Abreu[16], W. Adam[42], F. Adami[33], T. Adye[31], T. Akesson[19], G.D. Alekseev[12], P. Allen[41], S. Almehed[19], F. Alted[41], S.J. Alvsvaag[4], U. Amaldi[7], E. Anassontzis[3], P. Antilogus[20], W.-D. Apel[13], B. Åsman[37], J.-E. Augustin[15], A. Augustinus[7], P. Baillon[7], P. Bambade[15], F. Barao[16], G. Barbiellini[39], D.Y. Bardin[12], A. Baroncelli[34], O. Barring[19], W. Bartl[42], M. Battaglia[24], M.J. Bates[29], M. Baubillier[18], K.-H. Becks[44], C.J. Beeston[29], M. Begalli[10],P. Beiliere[6], Yu. Belokopytov[36], P. Beltran[9], D. Benedic[8], J.M. Benlloch[41], M. Berggren[37], D. Bertrand[2], S. Biagi[17], F. Bianchi[38], J.H. Bibby[29], M.S. Bilenky[12], P. Billoir[18], J. Bjarne[19], D. Bloch[8], S. Blyth[29], P.N. Bogolubov[12], T. Bolognese[33], M. Bonapart[26], M. Bonesini[24], P.S.L. Booth[17], M. Boratav[18], P. Borgeaud[33], H. Borner[29], C. Bosio[34], O. Botner[40], B. Bouquet[15], M. Bozzo[19], S. Braibant[7], P. Branchini[34], K.D. Brand[30], R.A. Brenner[11], C. Bricman[2], R.C.A. Brown[7], N. Brummer[26], J.-M. Brunet[6], L. Bugge[28], T. Buran[28], H. Burmeister[7], J.A.M.A. Buytaert[2], M. Caccia[7], M. Calvi[24], A.J. Camacho Rozas[35], J.-E. Campagne[7], A. Campion[17], T. Camporesi[7], V. Canale[32], F. Cao[2], L. Carroll[17], C. Caso[10], E. Castelli[39], M.V. Castillo Gimenez[41], A. Cattai[7], F.R. Cavallo[5], L. Cerrito[32], M. Chapkin[36], P. Charpentier[7], P. Checchia[30], G.A. Chelkov[12], L. Chevalier[33], P. Chliapnikov[36], V. Chorowicz[18], R. Cirio[38], M.P. Clara[38], P. Collins[29], J.L. Contreras[21], R. Contri[10], G. Cosme[15],F. Couchot[15], H.B. Crawley[1], D. Crennell[31], G. Crosetti[10], N. Crosland[29], M. Crozon[6], J. Cuevas Maestro[35], S. Czellar[11], S. Dagoret[15], E. Dahl-Jensen[25], B. Dalmagne[15], M. Dam[7], G. Damgaard[25], G. Darbo[10], E. Daubie[2], P.D. Dauncey[29], M. Davenport[7], P. David[18], A. D Angelis[39], M. DeBeer[33], H. DeBoeck[2], W. DeBoer[13],C. DeClercq[2], M.D.M. De Fez Laso[41], N. DeGroot[26], C. De La Vaissiere[18], B. DeLotto[39], C. Defoix[6], D. Delikaris[7], S. Delorme[7], P. Delpierre[6], N. Demaria[38], A. Demin[24], A. Demin[24], J. Derkaoui[38, 22], L. DiCiaccio[32], I. Dijkstra[7], F. Djama[8], J. Dolbeau[6], M. Donszelmann[26], K. Doroba[43], M. Dracos[7], J. Drees[44], M. Dris[27], W. Dulinski[8], R. Dzehlyadin[36], L.-O. Eek[40], P.A.-M. Eerola[11], T. Ekelof[40], G. Ekspong[37], A. Elliot Peisert[30], J.-P. Engel[8], D. Fassouliotis[27], M. Fernandez Alonso[35], A. Ferrer[41], T.A. Filippas[27], A. Firestone[1], H. Foeth[7], E. Fokitis[27], P. Folegati[39], F. Fontanelli[10], H. Forsbach[44], B. Franek[31], K.E. Fransson[40], P. Frenkiel[6], D.C. Fries[13], A.G. Frodesen[4], R. Fruhwirth[42], F. Fulda-Quenzer[15], K. Furnival[17], H. Furstenau[13], J. Fuster[7], J.M. Gago[16], G. Galeazzi[30], D. Gamba[38], C. Garcia[41], J. Garcia[35], U. Gasparini[30], P. Gavillet[7], E.N. Gazis[27], J.-P. Gerber[8], P. Giacomelli[5], K.-W. Glitza[44], R. Gokieli[7], V.M. Golovatyuk[12], J.J. Gomez Y Cadenas[7], A. Goobar[37], G. Gopal[31], M. Gorski[43], V. Gracco[10], A. Grant[7], F. Grard[2], E. Graziani[34], M.-H. Gros[15], G. Grosdidier[15], B. Grossetete[18], J. Guy[31], F. Hahn[7], M. Hahn[13], S. Haider[26], Z. Hajduk[26], A. Hakansson[19], A. Hallgren[40], K. Hamacher[44], G. Hamel De Monchenault[33], F.J. Harris[29], B.W. Heck[7], I. Herbst[44], J.J. Hernandez[41], P. Herquet[2], H. Herr[7], I. Hietanen[11], E. Higon[41], H.J. Hilke[7], S.D. Hodgson[29], T. Hofmokl[43], R. Holmes[1], S.-O. Holmgren[37], D. Holthuizen[26], P.F. Honore[6], J.E. Hooper[25], M. Houlden[17], J. Hrubec[42], P.O. Hulth[37], K. Hultqvist[37], D. Husson[8], B.D. Hyams[7], P. Ioannou[3], D. Isenhower[7], P.-S. Iversen[4], J.N. Jackson[17], P. Jalocha[14], G. Jarlskog[19], P. Jarry[33], B. Jean-Marie[15], E.K. Johansson[37], D. Johnson[17], M. Jonker[7], L. Jonsson[19], P. Jullot[8], G. Kalkanis[3], G. Kalmus[31], G. Kantardjian[7], F. Kapusta[18], P. Kapusta[14], S. Katsanevas[3], E.C. Katsoufis[27], R. Keranen[11], J. Kesteman[2], B.A. Khomenko[12], N.N. Khovanski[12], B. King[17], N.J. Kjaer[25], H. Klein[7], W. Klempt[7], A. Klovning[4], P. Kluit[26], J.H. Koehne[13], B. Koene[26], P. Kokkinias[9], M. Kopf[13], M. Koratzinos[7], K. Korcyl[14], A.V. Korytov[12], B. Korzen[7], V. Kostukhin[36], C. Kourkoumelis[3], T. Kreuzberger[42], J. Krolikowski[43], U. Kruener-Marquis[44], W. Krupinski[14], W. Kucewicz[24], K. Kurvinen[11], C. Lambropoulos[9], J.W. Lamsa[1], L. Lanceri[39], V. Lapin[36], J.-P. Laugier[33], R. Lauhakangas[11], G. Leder[42], F. Ledroit[6], J. Lemonne[2], G. Lenzen[44], V. Lepeltier[15], A. Letessier-Selvon[18], D. Liko[42], E. Lieb[44], E. Lillethun[4], J. Lindgren[11], A. Lipniacka[43], I. Lippi[30], R. Llosa[21], B. Loerstad[19], M. Lokajicek[12], J.G. Loken[29], M.A. Lopez Aguera[35], A. Lopez-Fernandez[15], M. Los[26], D. Loukas[9], A. Lounis[8], J.J. Lonzano[41], R. Lucock[31], P. Lutz[6], L. Lyons[29], G. Maehlum[7], J. Maillard[6], A. Maltezos[9], S. Maltezos[27], F. Mandl[42], J. Marco[35], M. Margoni[30], J.-C. Marin[7], A. Markou[9], L. Mathis[6], F. Matorras[35], C. Matteuzzi[24], G. Matthiae[32], M. Mazzucato[30], M. McCubbin[17], R. McKay[1], R. McNulty[17], E. Menichetti[38], G. Meola[10], C. Meroni[24], W.T. Meyer[1], M. Michelotto[30], W.A. Mitaroff[42], G.V. Mitselmakher[12], U. Mjoernmark[19], T. Moa[37], R. Moeller[25], K. Moenig[44], M.R. Monge[10], P. Morettini[10], H. Mueller[13], H. Muller[7], W.J. Murray[31], G. Myatt[29], F. Naraghi[18], U. Nau-Korzen[44], F.L. Navarria[5], P. Negri[24], B.S. Nielsen[25], B. Nijjhar[17], V. Nikolaenko[36], V. Obraztsov[36], A.G. Olshevski[12], R. Orava[11], A. Ostankow[36], A. Ouraou[33], R. Pain[18], H. Palka[26], T. Papadopoulou[27], L. Pape[7], A. Passeri[34], M. Pegoraro[30], V. Perevozchikov[36], M. Pernicka[42], A. Perrotta[5], F. Pierre[33], M. Pimenta[16], O. Pingot[2], A. Pinsent[29], M.E. Pol[16], G. Polok[14], P. Poropat[39], P. Privitera[13], A. Pullia[24],

---

272

J. Pyyhtia[11], D. Radojicic[29], S. Ragazzi[24], W.H. Range[17], P.N. Ratoff[29], A.L. Read[28], N.G. Redaelli[24],
M. Regler[42], D. Reid[17], P.B. Renton[29], L.K. Resvanis[3], F. Richard[15], M. Richardson[17], J. Ridky[12], G. Rinaudo[38],
I. Roditi[7], A. Romero[28], I. Roncagliolo[10], P. Ronchese[30], C. Ronnqvist[11], E.I. Rosenberg[1], U. Rossi[5], E. Rosso[7],
P. Roudeau[15], T. Rovelli[5], W. Ruckstuhl[26], V. Ruhlmann[33], A. Ruiz[35], K. Rybicki[14], H. Saarikko[11], Y. Sacquin[33],
J. Salt[41], E. Sanchez[41], J. Sanchez[21], M. Sannino[10], M. Schaeffer[8], H. Schneider[13], F. Scuri[39], A.M. Segar[29],
R. Sekulin[31], M. Sessa[39], G. Sette[10], R. Seufert[13], R.C. Shellard[16], P. Siegrist[33], S. Simonetti[10], F. Simonetto[30],
A.N. Sissakian[12], T.B. Skaali[28], G. Skjevling[28], G. Smadja[33, 20], G.R. Smith[31], N. Smirnov[36], R. Sosnowski[43],
T.S. Spassoff[12], E. Spiriti[34], S. Squarcia[10], H. Staeck[44], C. Stanescu[34], G. Stavropoulos[9], F. Stichelbaut[2], A. Stocchi[??],
J. Strauss[42], R. Strub[8], C.J. Stubenrauch[7], M. Szczekowski[43], M. Szeptycka[43], P. Szymanski[43], T. Tabarelli[24],
S. Tavernier[2], G. Theodosiou[9], A. Tilquin[23], J. Timmermans[26], V.G. Timoveev[12], L.G. Tkatchev[12], T. Todorov[12],
D.Z. Toet[26], Tomaradze[36], L. Tortora[34], M.T. Trainor[29], D. Treille[7], U. Trevisan[10], W. Trischuk[7], G. Tristam[6],
C. Troncon[24], A. Tsirou[7], E.N. Tsyganov[12], M. Turala[14], R. Turchetta[8], M.-L. Turluer[33], T. Tuuva[11], I.A. Tyapkin[12],
M. Tyndel[31], S. Tzamarias[7], S. Ueberschaer[44], O. Ullaland[7], V.A. Uvarov[36], G. Valenti[5], J.A. Valls Ferrer[41],
G.W. Van Apeldoorn[26], P. Van Dam[26], W.K. Van Doninck[2], N. Van Eijndhoven[7], C. Vander Velde[2], J. Varela[16]
P. Vaz[16], G. Vegni[24], J. Velasco[41], L. Ventura[30], W. Venus[31], F. Verbeure[2], L.S. Vertogradov[12], L. Vibert[18],
D. Vilanova[33], N. Vishnevsky[36], E.V. Vlasov[36], A.S. Vodopyanov[12], M. Vollmer[44], S. Volponi[5], G. Voulgaris[3],
M. Voutilainen[11], V. Vrba[34], H. Wahlen[44], C. Walck[37], F. Waldner[39], M. Wayne[1], P. Weilhammer[7], J. Werner[44],
A.M. Wetherell[7], J.H. Wickens[2], J. Wikne[28], G.R. Wilkinson[29], W.S.C. Williams[29], M. Winter[8], D. Wormald[28],
G. Wormser[15], K. Woschnagg[40], N. Yamdagni[37], P. Yepes[7], A. Zaitsev[36], A. Zalewska[14], P. Zalewski[43],
E. Zevgolatakos[9], G. Zhang[44], N.I. Zimin[12], M. Zito[33], R. Zitoun[18], R. Zukanovich Funchal[6], G. Zumerle[30], J. Zuniga[41]

[1] Ames Laboratory and Department of Physics, Iowa State University, Ames IA 50011, USA
[2] Physics Department, Univ. Instelling Antwerpen, Universiteitsplein 1, B-2610 Wilrijk, Belgium and IIHE, ULB-VUB, Pleinlaan 2, B-1050 Brussels, Belgium and Service de Phys. Des Part. Elém., Faculté des Sciences, Université de l'Etat Mons, Av. Maistriau 19, B-7000 Mons, Belgium
[3] Physics Laboratory, University of Athens, Solonos Str. 104, GR-10680 Athens, Greece
[4] Department of Physics, University of Bergen, Allégaten 55, N-5007 Bergen, Norway
[5] Dipartimento di Fisica, Università, di Bologna and INFN, Via Irnerio 46, I-40126 Bologna, Italy
[6] Collége de France, Lab. de Physique Corpusculaire, 11 pl. M. Berthelot, F-75231 Paris Cedex 05, France
[7] CERN, CH-1211 Geneva 23, Switzerland
[8] Division des Hautes Energies, CRN-Groupe DELPHI and LEPSI, B.P.20 CRO, F-67037 Strasbourg Cedex, France
[9] Institute of Nuclear Physics, N.R.C. Demokritos, P.O. Box 60628, GR-15310 Athens, Greece
[10] Dipartimento di Fisica, Università di Genova and INFN, Via Dodecaneso 33, I-16146 Genova, Italy
[11] Research Institute for High Energy Physics, University of Helsinki, Siltavouorenpenger 20 C, SF-00170 Helsinki 17, Finland
[12] Joint Institute for Nuclear Research, Dubna, Head Post Office, P.O. Box 79, SU-101 000 Moscow, USSR
[13] Institut für Experimentelle Kernphysik, Universität Karlsruhe, Postfach 6980, W-7500 Karlsruhe 1, Federal Republic of Germany
[14] High Energy Physics Laboratory, Institute of Nuclear Physics, Ul. Kawiory 26a, PL-30055 Krakow 30, Poland
[15] Université de Paris-Sud, Lab. de l'Accélérateur Lineaire, Bat 200, F-91405 Orsay, France
[16] LIP, Av. Elias Garcia 14-1e, P-1000 Lisbon Codex, Portugal
[17] Department of Physics, University of Liverpool, P.O. Box 147, Liverpool L69 3BX, UK
[18] LPNHE, Université Paris VI et VII, Tour 33 (RDC), 4 place Jussieu, F.-75230 Paris Cedex 05, France
[19] Department of Physics, University of Lund, Sölvegatan 14, S-22363 Lund, Sweden
[20] Université Claude Bernard de Lyon, 43 Bd du 11 Novembre 1918, F-69622 Villeurbanne Cedex, France
[21] Departamento de Fisica Atomica Molecular y Nuclear, Universidad Complutense, Avda. Complutense s/n, E-28040 Madrid, Spain
[22] Permanent address: Départment de Physique, Faculté des Sciences d'Oujda, Maroc
[23] Faculté des Sciences de Luminy, Univ. d'Aix – Marseille II Case 907 – 70, route Léon Lachamp, F-13288 Marseille Cedex 09, France
[24] Dipartimento di Fisica, Unversità di Milano and INFN, Via Celoria 16, I-20133 Milan, Italy
[25] Niels Bohr Institute, Blegdamsvej 17, DK-2100 Copenhagen O, Denmark
[26] NIKHEF-H, Postbus 41882, NL-1009 DB Amsterdam, The Netherlands
[27] National Technical University, Physics Department, Zografou Campus, GR-15773 Athens, Greece
[28] Physics Department, University of Oslo, Blindern, N-1000 Oslo 3, Norway
[29] Nuclear Physics Laboratory, University of Oxford, Keble Road, Oxford OX1 3RH, UK
[30] Dipartimento di Fisica, Università di Padova and INFN, Via Marzolo 8, I-35131 Padua, Italy
[31] Rutherford Appleton Laboratory, Chilton, Didcot OX11 OQX, UK
[32] Dipartimento di Fisica, Università di Roma II and INFN, Tor Vergata, I-00173 Rome, Italy
[33] CEN-Saclay, DPhPE, F-91191 Gif-sur-Yvette Cedex, France
[34] Istituto Superiore di Sanità, Ist. Naz. di Fisica Nucl. (INFN), Viale Regina Elena 299, I-00161 Rome, Italy
[35] Facultad de Ciencias, Universidad de Santander, av. de los Casatros, E-39005 Santander, Spain
[36] Institute for High Energy Physics, Serpukow P.O. Box 35, Protvino, (Moscow Region), USSR
[37] Institute of Physics, University of Stockholm, Vanadisvägen 9, S-113 46 Stockholm, Sweden
[38] Dipartimento di Fisica Sperimentale, Università di Torino and INFN, Via P. Giuria 1, I-10125 Turin, Italy
[39] Dipartimento di Fisica, Università di Trieste and INFN, Via A. Valerio 2, I-34127 Trieste, Italy and Istituto di Fisica, Università di Udine, I-33100 Udine, Italy
[40] Department of Radiation Sciences, University of Uppsala, P.O. Box 535, S-751 21 Uppsala, Sweden
[41] Inst. de Fisica Corpuscular IFIC, Centro Mixto Univ. de Valencia-CSIC, Avda. Dr. Moliner 50, E-46100 Burjassot (Valencia), Spain
[42] Institut für Hochenergiephysik, Oesterreich Akad. d. Wissensch., Nikolsdorfergasse 18, A-1050 Vienna, Austria
[43] Inst. Nuclear Studies and, University of Warsaw, U. Hoza 69, PL-00681 Warsaw, Poland
[44] Fachbereich Physik, University of Wuppertal, Postfach 100 127, W-5600 Wuppertal 1, Federal Republic of Germany

Abstract. The multiplicity distributions of charged particles in restricted rapidity intervals in Z^0 hadronic decays measured by the DELPHI detector are presented. The data reveal a shoulder structure, best visible for intervals of intermediate size, i.e. for rapidity limits around ± 1.5. The whole set of distributions including the shoulder structure is reproduced by the Lund Parton Shower model. The structure is found to be due to important contributions from 3- and 4-jet events with a hard gluon jet. A different model, based on the concept of independently produced groups of particles, "clans", fluctuating both in number per event and particle content per clan, has also been used to analyse the present data. The results show that for each interval of rapidity the average number of clans per event is approximately the same as at lower energies.

1 Introduction

In a recent paper [1] we presented an analysis of the multiplicity distribution of charged particles produced in Z^0 hadronic decays in the DELPHI detector at CERN.

To learn more about the mechanisms of multiparticle production we extend here this study and report on properties of the charged particle multiplicity distributions in restricted intervals of rapidity. The data are compared with the predictions of the Lund Parton Shower model (Monte Carlo program JETSET version 6.3) [2, 3]. The comparisons were made after transforming the model predictions for the number of charged particles to the corresponding predictions for the number of tracks expected in the DELPHI detector. The second model studied, which is based on the negative binomial distribution, was treated similarly. In this case the two free parameters of the model were adjusted to fit the data. One interpretation of this distribution [4–6] is based on the concept of independently produced groups of particles, "clans", fluctuating in number per event with a group membership fluctuating such that the resulting charged particle distribution is a negative binomial distribution.

In Sect. 2 the event sample, the selection criteria and correction procedures are described. Experimental results on multiplicity distributions are presented in Sect. 3, while a summary of the main conclusions is given in Sect. 4.

2 Selection and treatment of data

This study is based on 94439 hadronic events with $n_{ch} \geq 5$ obtained in 1989–1990 with the DELPHI detector at the LEP collider at energies near the Z^0-resonance. The DELPHI detector has been described in detail elsewhere [7]. The measurements presented here are based on the charged particles detected by the Time Projection Chamber (TPC). For event selection, we apply the same cuts as in the DELPHI-study [1] on charged particle multiplicity distribution. The most important of these cuts are: tracks were kept only if they extrapolated back to the

nominal crossing point within $\Delta r < 5$ cm and $\Delta z < 10$ cm, if their momentum was greater 0.1 GeV/c, if the measured track length was above 50 cm and if the polar angle was between $25°$ and $155°$. Events were kept only if the energy of charged particles (assumed to have pion mass) in each of the two hemispheres with respect to the beam axis exceeded 3 GeV, if the total energy of charged particles exceeded 15 GeV, if there were at least 5 charged particles with momenta above 0.2 GeV/c and if the polar angle of the sphericity axis was in the range $40° < \theta < 140°$. The resulting data sample comprised 63434 events. The possible contaminations from events due to beam-gas scattering, $\gamma\gamma$ interactions and $\tau^+\tau^-$ events, were reduced to a negligible level ($< 0.1\%$, $< 0.1\%$ and $< 0.15\%$, respectively) by the imposed cuts.

The correction procedure and the treatment of systematic uncertainties were the same as those used earlier [1]. The acceptance matrix of the detector, including the imposed cuts, was determined from a full detector simulation of 54000 events generated according to the Lund Parton Shower (PS) model (Monte Carlo program JETSET version 6.3) [2, 3]. The treatment of the simulated tracks was done in the same way as the real data. Let $N_{obs}(m)$ be the number of accepted events with m tracks when the corresponding number of produced events, $N_{tr}(n)$, had n charged particles. Any complete loss of events due to inefficiencies has to be treated separately, i.e. the $N_{tr}(n)$ here is in fact the product of the acceptance efficiency and the total number of produced events. The acceptance matrix is then given by $M(m,n) = N_{obs}(m)/N_{tr}(n)$. For fixed n the matrix elements are in practice non-zero only for a limited interval in m, the size of which depends on n. For fixed n it holds that $\sum_m M(m,n) = 1$, implying that the matrix element is the probability that an accepted event with n produced charged particles appears as an event with m tracks. This matrix is independent of the shape of the multiplicity distribution produced by the model and can be used for any other multiplicity distribution, provided the kinematics of produced charged particles do not differ widely from the kinematics of the Lund PS model.

Using normalized probability distributions for produced charged particles $P_{tr}(n)$ and for accepted events $P_{obs}(m)$ the relation between them is

$$P_{obs}(m) = \sum_n M(m,n) \cdot P_{tr}(n). \tag{1}$$

Obviously $f(n,m) = M(m,n) \cdot P_{tr}(n)/P_{obs}(m)$ is the fraction of the population in bin m which came from bin n. By construction one may recover the true $P_{tr}(n)$ distribution by the operation

$$P_{tr}(n) = \sum_m f(n,m) \cdot P_{obs}(m). \tag{2}$$

The basic assumption made is that the same fraction holds also for the case when the true distribution in produced charged particles $T(n)$ is to be recovered from an experimentally observed multiplicity distribution of tracks, $O(m)$. Thus the assumption leads to

$$T(n) = \sum_m M^T(n,m) \cdot (P_{tr}(n)/P_{obs}(m)) \cdot O(m),$$

or

$$T(n)/P_{tr}(n) = \sum_m M^T(n,m) \cdot O(m)/P_{obs}(m), \qquad (3)$$

where M^T is the transpose of the matrix M. One may write the two basic relations, (1) and (3), in matrix notation as follows

$$P_{obs} = M \cdot P_{tr}, \qquad (4)$$

and

$$\tau = M^T \cdot \omega, \qquad (5)$$

where the vector of ratios $\tau(n) = T(n)/P_{tr}(n)$ and $\omega(m) = O(m)/P_{obs}(m)$ have been introduced. If the model predictions are equal to the observed data the solution according to (3) will be equal to the model. If the model predictions are close to the data, the corrections will not be large. Since it is advantageous to have only small corrections, one should prefer to base the recovery of the true distribution on a good model. The amount of agreement between the model and the data is measured by calculating the χ^2 between $O(m)$ and $P_{obs}(m)$, both normalised to the actual sample size and also by observing the sign-changes in the set of differences. It should be remarked that the matrix M had to be found for each rapidity interval under study.

3 Experimental results

The multiplicity distributions are given in Table 1 for different rapidity intervals (rapidity was calculated with respect to the thrust axis assuming pion mass for all particles). The Table contains data with particles emitted in central rapidity intervals as well as the subset of particles emitted in a single hemisphere, defined by the plane perpendicular to the thrust axis. In the latter case the rapidity intervals were extended to $|y| < 5.0$, whereas in the first case it is restricted to $|y| < 2.0$ in order to avoid odd-even effects due to charge conservation, visible at the larger rapidity intervals. Charge conservation restricts the multiplicities to even values only for the case of the full phase space.

The quoted errors here and elsewhere are calculated from the statistical errors and from the correction procedure as described in [1]. It should be pointed out that the errors given in Table 1 are strongly correlated for nearby bins due to the method of correction. The multiplicity distributions are also presented in Fig. 1 and, in the KNO-form [8] ($\psi(z) = \langle n \rangle P(n)$ versus $z = n/\langle n \rangle$), in Fig. 2. Except for the distribution of charged particles in full phase space, odd and even topologies are plotted consecutively. For clarity, each successive distribution in Figs. 1 and 2 is lowered by a factor of ten.

From Fig. 1 it is seen that the multiplicity distribution becomes narrower as the rapidity interval is reduced. On the contrary, the distribution in KNO-form (Fig. 2) wid-

Table 1a–h. Corrected charged particle multiplicity distributions $P(n) \times 10^3$ in central rapidity (y) intervals and in a single hemisphere. The errors in nearby bins are strongly correlated

n	a) $|y| < 0.5$ both hem.		sing. hem.		b) $|y| < 1.0$ both hem.		sing. hem.	
0	116	±5	301	±12	20	±1	116	±5
1	192	±8	299	±12	56	±2	193	±8
2	198	±8	191	±8	93	±4	195	±8
3	158	±7	101	±4	116	±5	155	±6
4	108	±5	51	±2	121	±5	108	±5
5	73	±3	26	±1	111	±5	73	±3
6	50	±2	14.5	±0.7	93	±4	47	±2
7	34	±2	7.9	±0.5	77	±3	33	±2
8	23	±1	4.2	±0.3	62	±3	22	±1
9	15.9	±0.8	2.3	±0.2	51	±2	15.3	±0.8
10	11.2	±0.6	1.0	±0.1	40	±2	11.8	±0.6
11	7.2	±0.4	0.56	±0.09	32	±1	8.7	±0.5
12	4.6	±0.3	0.25	±0.06	26	±1	6.3	±0.4
13	3.3	±0.3	0.16	±0.05	22	±1	4.6	±0.3
14	2.0	±0.2	0.05	±0.03	15.7	±0.8	3.3	±0.3
15	1.2	±0.1	0.04	±0.02	13.9	±0.7	2.2	±0.2
16	0.9	±0.1			9.7	±0.5	2.1	±0.2
17	0.57	±0.09			9.0	±0.5	1.3	±0.2
18	0.36	±0.07			7.3	±0.4	1.0	±0.1
19	0.19	±0.05			5.8	±0.4	0.54	±0.09
20	0.05	±0.03			4.6	±0.3	0.43	±0.08
21	0.03	±0.02			4.1	±0.3	0.28	±0.06
22					2.9	±0.2	0.22	±0.06
23					2.1	±0.2	0.10	±0.04
24					1.9	±0.2	0.03	±0.02
25					1.2	±0.1	0.02	±0.02
26					0.9	±0.1	0.05	±0.03
27					0.7	±0.1	0.03	±0.02
28					0.56	±0.09	0.02	±0.02
29					0.43	±0.08		
30					0.17	±0.05		
31					0.4	±0.2		
32					0.16	±0.05		
33					0.11	±0.04		
34					0.08	±0.03		
35					0.04	±0.02		

Table 1 (continued)

n	c) $|y| < 1.5$ both hem.		sing. hem.		d) $|y| < 2.0$ both hem.		sing. hem.	
0	4.1	±0.3	49	±2	0.9	±0.1	21	±1
1	13.7	±0.7	106	±4	3.7	±0.3	56	±2
2	32	±1	146	±6	9.3	±0.5	95	±4
3	51	±2	149	±6	18.6	±0.9	117	±5
4	70	±3	130	±5	31	±1	120	±5
5	84	±4	100	±4	44	±2	110	±5
6	88	±4	76	±3	56	±2	92	±4
7	86	±4	56	±2	66	±3	75	±3
8	80	±3	41	±2	68	±3	59	±3
9	72	±3	30	±1	69	±3	47	±2
10	61	±3	24	±1	67	±3	37	±2
11	52	±2	18.2	±0.9	63	±3	30	±1
12	45	±2	15.2	±0.8	57	±3	25	±1
13	38	±2	12.0	±0.6	52	±2	22	±1
14	33	±2	10.9	±0.6	46	±2	19.3	±0.9
15	29	±1	8.3	±0.5	43	±2	16.3	±0.8
16	24	±1	6.8	±0.4	38	±2	13.5	±0.7
17	21	±1	5.6	±0.4	35	±2	11.1	±0.6

Table 1 (continued)

n	c) $|y| < 1.5$ both hem.	sing. hem.	d) $|y| < 2.0$ both hem.	sing. hem.
18	18.6 ±0.9	4.0 ±0.3	30 ±1	8.5 ±0.5
19	16.3 ±0.8	3.4 ±0.3	28 ±1	6.8 ±0.4
20	13.6 ±0.7	2.6 ±0.2	25 ±1	5.1 ±0.3
21	11.9 ±0.6	1.9 ±0.2	22 ±1	4.2 ±0.3
22	9.8 ±0.5	1.4 ±0.2	20 ±1	3.0 ±0.2
23	8.7 ±0.5	1.0 ±0.1	18.3 ±0.9	2.1 ±0.2
24	7.2 ±0.4	0.6 ±0.1	15.0 ±0.8	1.5 ±0.2
25	5.6 ±0.4	0.47 ±0.08	12.6 ±0.7	1.0 ±0.1
26	5.1 ±0.3	0.21 ±0.06	10.7 ±0.6	0.7 ±0.1
27	4.2 ±0.3	0.14 ±0.04	9.2 ±0.5	0.45 ±0.08
28	3.5 ±0.3	0.06 ±0.03	8.2 ±0.5	0.30 ±0.07
29	2.7 ±0.2	0.05 ±0.03	7.2 ±0.4	0.09 ±0.04
30	2.6 ±0.2	0.07 ±0.03	5.5 ±0.4	0.08 ±0.04
31	1.8 ±0.2	0.03 ±0.02	4.7 ±0.3	0.07 ±0.03
32	1.1 ±0.1	0.008 ±0.008	4.0 ±0.3	0.04 ±0.02
33	1.1 ±0.1		3.4 ±0.3	0.008 ±0.008
34	1.0 ±0.1		2.5 ±0.2	
35	0.45 ±0.08		2.2 ±0.2	
36	0.8 ±0.3		1.3 ±0.1	
37	0.32 ±0.07		1.3 ±0.2	
38	0.2 ±0.1		1.1 ±0.1	
39	0.12 ±0.07		0.8 ±0.1	
40	0.25 ±0.06		0.7 ±0.1	
41	0.08 ±0.03		0.37 ±0.07	
42	0.02 ±0.02		0.28 ±0.06	
43	0.08 ±0.03		0.23 ±0.06	
44	0.06 ±0.03		0.15 ±0.05	
45			0.11 ±0.04	
46			0.13 ±0.04	
47			0.11 ±0.04	
48			0.02 ±0.02	

Table 1 (continued)

n	e) $|y| < 3.0$ sing. hem.	f) $|y| < 4.0$ sing. hem.	g) $|y| < 50$ sing. hem.
0	3.2 ±0.3	0.7 ±0.1	0.31 ±0.07
1	11.0 ±0.6	2.8 ±0.2	1.3 ±0.1
2	29 ±1	8.3 ±0.5	5.0 ±0.3
3	48 ±2	18.6 ±0.9	12.9 ±0.7
4	70 ±3	36 ±2	27 ±1
5	84 ±4	54 ±2	46 ±2
6	91 ±4	73 ±3	71 ±3
7	90 ±4	87 ±4	85 ±4
8	86 ±4	96 ±4	100 ±4
9	77 ±3	95 ±4	100 ±4
10	71 ±3	92 ±4	98 ±4
11	61 ±3	83 ±4	88 ±4
12	54 ±2	74 ±3	78 ±3
13	46 ±2	62 ±3	66 ±3
14	39 ±2	51 ±2	53 ±2
15	32 ±1	41 ±2	42 ±2
16	26 ±1	32 ±2	33 ±2
17	21 ±1	25 ±1	26 ±1
18	16.4 ±0.8	19.0 ±0.9	19.2 ±0.9
19	12.5 ±0.7	13.9 ±0.7	14.1 ±0.7
20	9.4 ±0.5	10.6 ±0.6	10.6 ±0.6
21	7.1 ±0.4	7.7 ±0.5	7.8 ±0.5
22	5.3 ±0.3	5.7 ±0.4	5.7 ±0.4
23	3.5 ±0.3	3.8 ±0.3	3.8 ±0.3
24	2.9 ±0.2	3.0 ±0.2	3.1 ±0.2
25	1.6 ±0.2	1.8 ±0.2	1.8 ±0.2

Table 1 (continued)

n	e) $|y| < 3.0$ sing. hem.	f) $|y| < 4.0$ sing. hem.	g) $|y| < 50$ sing. hem.
26	1.0 ±0.1	1.1 ±0.1	1.1 ±0.1
27	0.8 ±0.1	0.9 ±0.1	0.9 ±0.1
28	0.50 ±0.09	0.52 ±0.09	0.52 ±0.09
29	0.24 ±0.06	0.27 ±0.06	0.27 ±0.06
30	0.22 ±0.06	0.20 ±0.05	0.20 ±0.05
31	0.10 ±0.04	0.11 ±0.04	0.11 ±0.04
32	0.06 ±0.03	0.06 ±0.03	0.06 ±0.03
33	0.02 ±0.02	0.02 ±0.02	0.02 ±0.02
34	0.02 ±0.02	0.02 ±0.02	0.02 ±0.02

Table 1 (continued)

h) all y

n	both hem.	n	sing. hem.
0		0	0.19 ±0.05
2		1	1.2 ±0.1
4	0.18 ±0.05	2	4.6 ±0.3
6	1.4 ±0.2	3	12.2 ±0.6
8	6.6 ±0.4	4	27 ±1
10	22 ±1	5	46 ±2
12	48 ±2	6	71 ±3
14	81 ±3	7	85 ±4
16	110 ±5	8	100 ±4
18	127 ±5	9	100 ±4
20	130 ±5	10	99 ±4
22	119 ±5	11	88 ±4
24	100 ±4	12	78 ±3
26	78 ±3	13	66 ±3
28	60 ±3	14	53 ±2
30	41 ±2	15	42 ±2
32	29 ±1	16	33 ±2
34	18.5 ±0.9	17	26 ±1
36	12.4 ±0.7	18	19.2 ±0.9
38	7.7 ±0.5	19	14.1 ±0.7
40	4.3 ±0.3	20	10.6 ±0.6
42	2.3 ±0.2	21	7.8 ±0.5
44	1.3 ±0.2	22	5.7 ±0.4
46	0.8 ±0.1	23	3.8 ±0.3
48	0.26 ±0.06	24	3.1 ±0.2
50	0.26 ±0.07	25	1.8 ±0.2
52	0.10 ±0.04	26	1.1 ±0.1
		27	0.9 ±0.1
		28	0.52 ±0.09
		29	0.27 ±0.06
		30	0.20 ±0.05
		31	0.11 ±0.04
		32	0.06 ±0.03
		33	0.02 ±0.02
		34	0.02 ±0.02

ens under the same imposed cuts in rapidity. In Table 2 the average multiplicity $\langle n \rangle$, the dispersion D, defined by $D^2 = \langle n^2 \rangle - \langle n \rangle^2$, and the moments $C_q = \langle n^q \rangle / \langle n \rangle^q$ for $q = 2$ to 5 are presented. All moments C_q increase with decreasing size of the rapidity interval, reflecting the widening of the KNO multiplicity distribution.

The predictions of the Lund Parton Shower model are plotted together with the corrected data in Fig. 1. However, the judgment of the amount of agreement or disa-
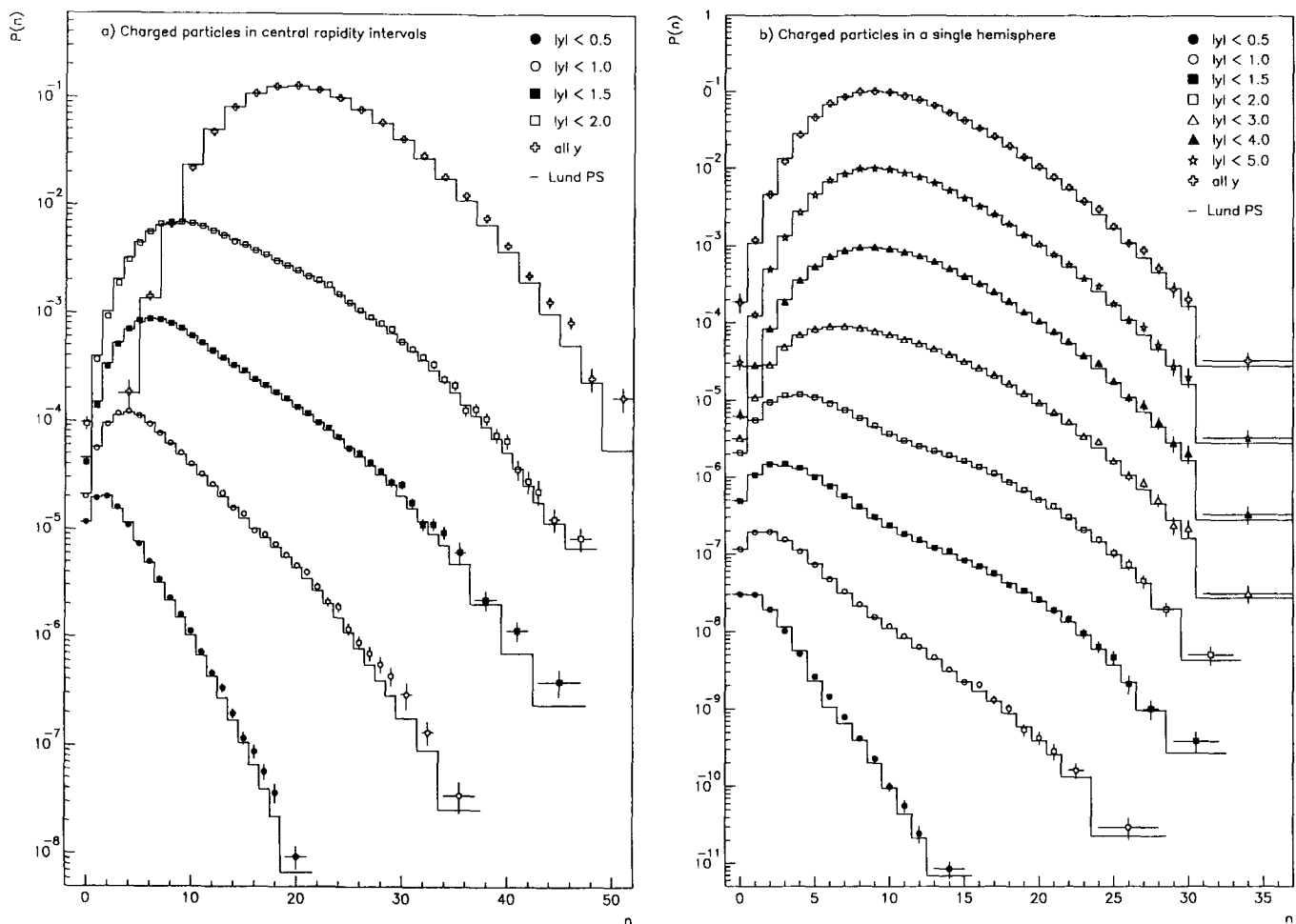
Fig. 1 a, b. Corrected charged particle multiplicity distributions $P(n)$ **a** in central rapidity intervals and **b** in a single hemisphere. Each successive distribution is lowered by a factor of ten. The histograms show the Lund PS model predictions
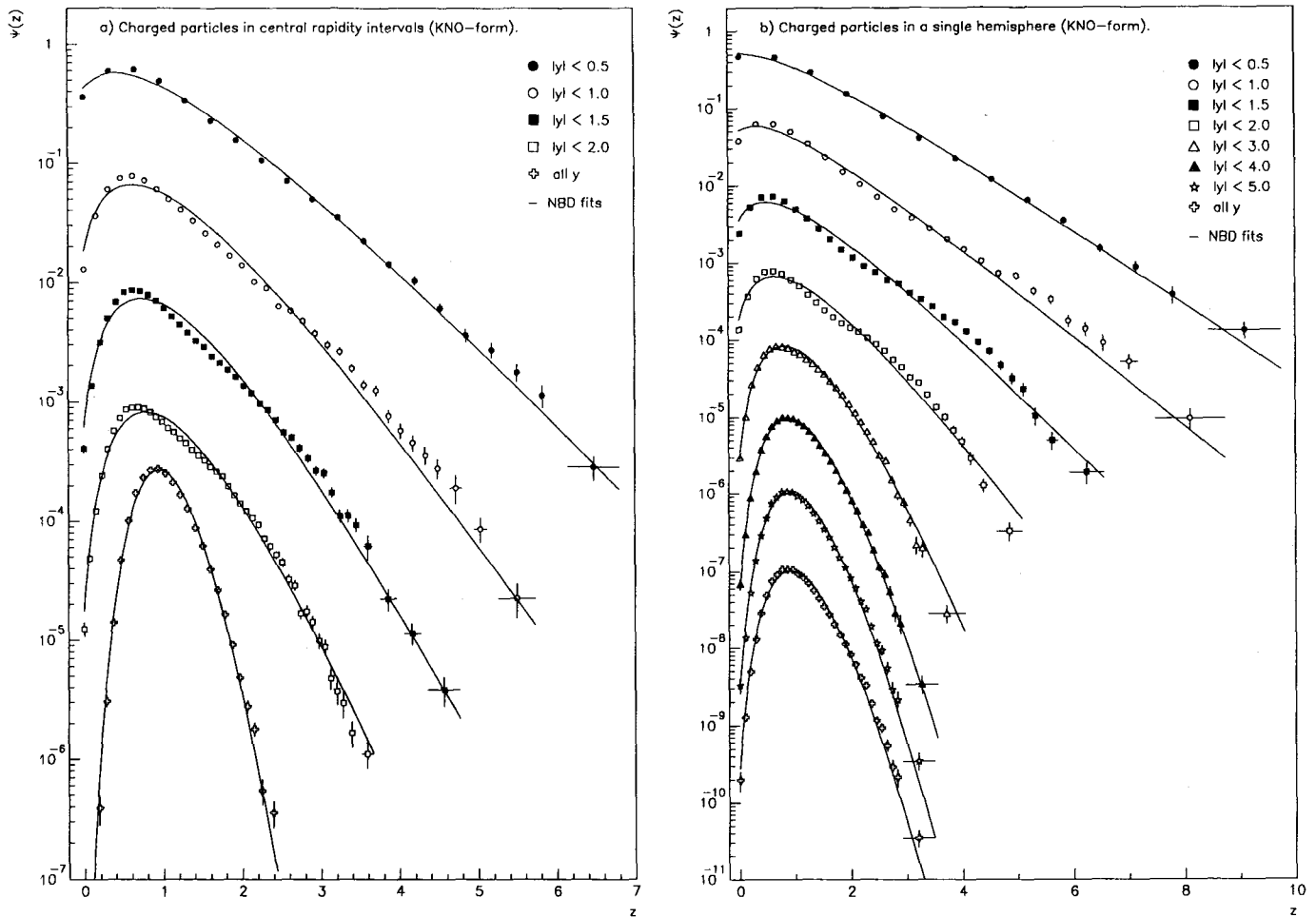
Table 2a, b. Moments of charge particle multiplicity distributions in central rapidity intervals and in a single hemisphere.

a) Charged particles in central rapidity intervals

$|y|$	$\langle n \rangle$	D	C_2	C_3	C_4	C_5
< 0.5	3.1 ± 0.1	2.7 ± 0.1	1.74 ± 0.07	4.2 ± 0.2	12.6 ± 0.6	45 ± 2
< 1.0	6.5 ± 0.3	4.6 ± 0.2	1.51 ± 0.06	3.1 ± 0.1	7.8 ± 0.3	23 ± 1
< 1.5	9.9 ± 0.4	6.2 ± 0.3	1.39 ± 0.06	2.5 ± 0.1	5.3 ± 0.2	12.9 ± 0.6
< 2.0	13.1 ± 0.5	7.1 ± 0.3	1.29 ± 0.05	2.03 ± 0.09	3.7 ± 0.2	7.5 ± 0.3
all	20.8 ± 0.8	6.2 ± 0.4	1.09 ± 0.03	1.29 ± 0.03	1.63 ± 0.04	2.20 ± 0.06

b) Charged particles in a single hemisphere

$|y|$	$\langle n \rangle$	D	C_2	C_3	C_4	C_5
< 0.5	1.54 ± 0.06	1.6 ± 0.1	2.14 ± 0.09	6.5 ± 0.3	26 ± 1	122 ± 7
< 1.0	3.2 ± 0.1	2.9 ± 0.1	1.84 ± 0.08	5.0 ± 0.2	17.5 ± 0.8	75 ± 4
< 1.5	4.9 ± 0.2	4.0 ± 0.2	1.67 ± 0.07	3.9 ± 0.2	11.5 ± 0.5	39 ± 4
< 2.0	6.5 ± 0.3	4.7 ± 0.2	1.51 ± 0.06	3.0 ± 0.1	7.2 ± 0.3	19.6 ± 0.9
< 3.0	9.2 ± 0.4	4.8 ± 0.2	1.28 ± 0.05	1.94 ± 0.08	3.4 ± 0.2	6.6 ± 0.3
< 4.0	10.2 ± 0.4	4.3 ± 0.3	1.18 ± 0.04	1.60 ± 0.06	2.4 ± 0.1	4.1 ± 0.2
< 5.0	10.4 ± 0.5	4.2 ± 0.3	1.16 ± 0.03	1.54 ± 0.04	2.29 ± 0.06	3.8 ± 0.1
all	10.4 ± 0.5	4.2 ± 0.3	1.16 ± 0.03	1.54 ± 0.04	2.28 ± 0.06	3.7 ± 0.1

Fig. 2. The same as in Fig. 1 but in KNO-form of $\psi(z) = \langle n \rangle P(n)$ *versus* $z = n/\langle n \rangle$. The solid curves represent the negative binomial distributions with parameters obtained from the data

Table 3a, b. The values of χ^2/NDF obtained from differences between the uncorrected multiplicity distributions and the predictions of the Lund PS model and from the predictions from fitted negative binomial distributions. The model distributions were transformed according to the matrix relation $P_{\text{PRED}} = M \cdot P_{\text{MOD}}$, see (1) or (4)

a) Charged particles in central rapidity intervals

$\|y\|$	Lund PS	NBD
< 0.5	55/20	75/18
< 1.0	67/32	342/30
< 1.5	81/42	478/40
< 2.0	68/46	280/44
all	81/43	205/41

b) Charged particles in a single hemisphere

$\|y\|$	Lund PS	NBD
< 0.5	37/16	39/14
< 1.0	48/26	287/24
< 1.5	56/31	530/29
< 2.0	42/33	472/31
< 3.0	59/35	143/33
< 4.0	68/35	45/33
< 5.0	82/35	151/33
all	89/35	174/33

greement has been made between the transformed predictions for frequencies of track-multiplicities and the raw, uncorrected data. For the subset of particles in a single hemisphere the χ^2-probabilities (see Table 3) are small and the number of sign-changes are too few to make the agreements good. For the case of full phase space both the χ^2-values and the number of sign changes indicate rather poor agreement between the Lund PS predictions and the data. However, the origin of all the observed disagreements are found to be due to systematic differences in the high multiplicity tails of the various distributions, such that the frequencies of events in the model predictions fall below the data. Because of the large sample size such differences cause noticable contributions to the χ^2.

The origin of these differences could be due to a failure of the model to produce sufficiently many high multiplicity events or due to a failure of the detector simulation by causing somewhat too large net losses when transforming the model data from the number of produced particles to the predicted number of tracks. If anything we would expect the simulation to cause too small losses. A detailed study of what would be needed to bring the

simulated model predictions into agreement with the data in the high multiplicity tail regions shows, that the present net losses are too large by about 0.5 particles per event, independent of whether the tail region is around 20, 30 or 40 particles. Such an independence of the primary multiplicity indicates that the simulation program is not causing the discrepancies. Thus it seems unavoidable to conclude that the Lund PS model slightly underestimates the frequencies of high multiplicity events. The Lund PS model is, however, describing the measured, uncorrected data sufficiently well so that the recovery of the true distributions as given in Table 1 and Fig. 1 has been based on it. The negative binomial distributions (NBD), with the two parameters taken from the data, represent less good models as seen from the χ^2-values in Table 3. However, when they are used as bases for the recovery of the true distributions the results are quite similar to the ones given in Table 1 and in Fig. 1.

An interesting feature of the data is a shoulder in the multiplicity distributions, best seen for intervals of rapidity $|y| < 1.5$ and $|y| < 2.0$ and most prominent for the case of single hemisphere data (Fig. 1b). This shoulder structure is present already in the raw, uncorrected data and is thus not an artifact created by the correction procedure. The Lund PS model predicts this shoulder structure rather well. In an attempt to understand this structure we resolved the data into multi-jet hadronic final states, using the jet finding algorithm originally introduced by the JADE collaboration [9] and recently applied by a number of other collaborations [10–12] for investigations of jet production rates at the Z^0-resonance. For each event the squares of the scaled invariant masses for each pair of charged particles i and j,

$$Y_{ij} = 2 E_i E_j (1 - \cos \theta_{ij})/E_{\mathrm{vis}}^2, \tag{6}$$

are evaluated. Here E_i, E_j are the energies and θ_{ij} the angle between the momentum vectors of the two particles, E_{vis} is the total charged energy of the event (pion mass assumed). The particle pair with the lowest value of Y_{ij} is selected and replaced by a pseudo-particle with four momentum $(p_i + p_j)$, hereby reducing the multiplicity by one. In successive steps the procedure is repeated until the values Y_{ij} for all pairs of pseudo-particles or particles are larger than a given jet cut resolution Y_{cut}. The remaining pseudo-particles or particles are called jets. The choice of the lower limit for the scaled invariant mass has arbitrarily and conventionally been set at $Y_{\mathrm{cut}} = 0.04$.

With this jet definition and as an illustration, the multiplicity distribution for the rapidity interval $|y| < 2$ has been resolved into components of 2-, 3- and 4-jet events as shown in Fig. 3a. The figure contains also the Lund PS model predictions obtained by using the same JADE jet finding algorithm and demonstrates rather good agreement between model and data, apart from a slight systematic underestimation of the high multiplicity tails and of the number of 4-jet events. The main features seen from Fig. 3a is that the multiplicity distribution is dominated by contributions from 2-jet events at low multiplicities with a peak at $n \approx 10$, has a shoulder at $n \approx 20$–25 due to 3-jet event contributions and has a tail dominated by 3- and 4-jet events. In Fig. 3b are given components due to $q\bar{q}$-, $q\bar{q}g$- and $q\bar{q}gg$-events as predicted by the JETSET 7.2 Monte Carlo program [3] with parameters optimized for the center-of-mass energy of 91 GeV [13], containing the second order QCD Matrix Elements (ME) of Gutbrod-Kramer-Schierholz [14]. The Lund ME model also describes the experimental data apart from a slight underestimation of the high multiplicity tail of the distribution (as seen also for the Lund PS in Fig. 3a) and an underestimation of the data at small n (not seen for the Lund PS in Fig. 3a). The contribution of $q\bar{q}$-events in the Lund ME model is rather small peaking at low multiplicities ($n \approx 7$) and it practically vanishes at $n > 20$. The $q\bar{q}g$-events give the most important contribution at the maximum of the experimental distribution at $n \approx 10$, while the $q\bar{q}gg$-events (and a small, $\approx 4.5\%$, admixture of $q\bar{q}q\bar{q}$-events) dominate the distribution at $n \geq 20$ and explain the shoulder structure.

The dominance of the multi-jet events at large multiplicities explains why the structure in multiplicity distributions is best seen in the central rapidity windows with $|y| < 1.5, 2$. Indeed, the multi-jet events are more "spherical" with respect to the thrust axis and therefore imposed cuts on rapidity reduce the multiplicities of multi-jet events much less than those of 2-jet events, thereby enhancing the difference between their respective average multiplicities. The differences between the multiplicity distributions of 2-, 3- and 4-jet events explain also why the shoulder structure is most prominent for the case of single hemisphere data.

In the multiplicity distribution for $\bar{p}p$-collisions at 900 GeV c.m. energy the UA5 collboration [15] observed a narrow peak and a shoulder-like structure. This peculiar shape was reported to depend on the size of the pseudorapidity interval, being most pronounced for large and disappear for small intervals. This is different from what we here observe in e^+e^- collisions.

The UA5 collaboration has also observed that the NBD, which was successfully fitted to the charged multiplicity distributions in full phase space and in limited parts of it for various interactions [16–25], fails to give a good fit to data at the center-of-mass energy of 900 GeV [15] in full phase space and for large rapidity intervals due to a shoulder structure. The fit of the NBD to our data in restricted rapidity intervals is found to be of rather poor quality (see Fig. 2 and χ^2/NDF values in Table 3) due to the shoulder structure of the experimental distributions. The maximum amplitudes of the deviations between the NBD model predictions and the data amount to about 15 to 20% (30% for a single hemisphere). Obviously, a superposition of two or more NBD's would fit the data better, but we do not pursue this approach here. However, the gross shapes of the experimental distributions including the tails at high multiplicities are reasonably well reproduced. Therefore, and since several earlier investigations have been performed along these lines, we also analyse our data in terms of the "clan" cascading picture, introduced independently by Ekspong [4] and Giovannini and Van Hove [5, 6]. The term "clan" refers to a group of particles with common and independently produced ancestor, the number of which per event there-
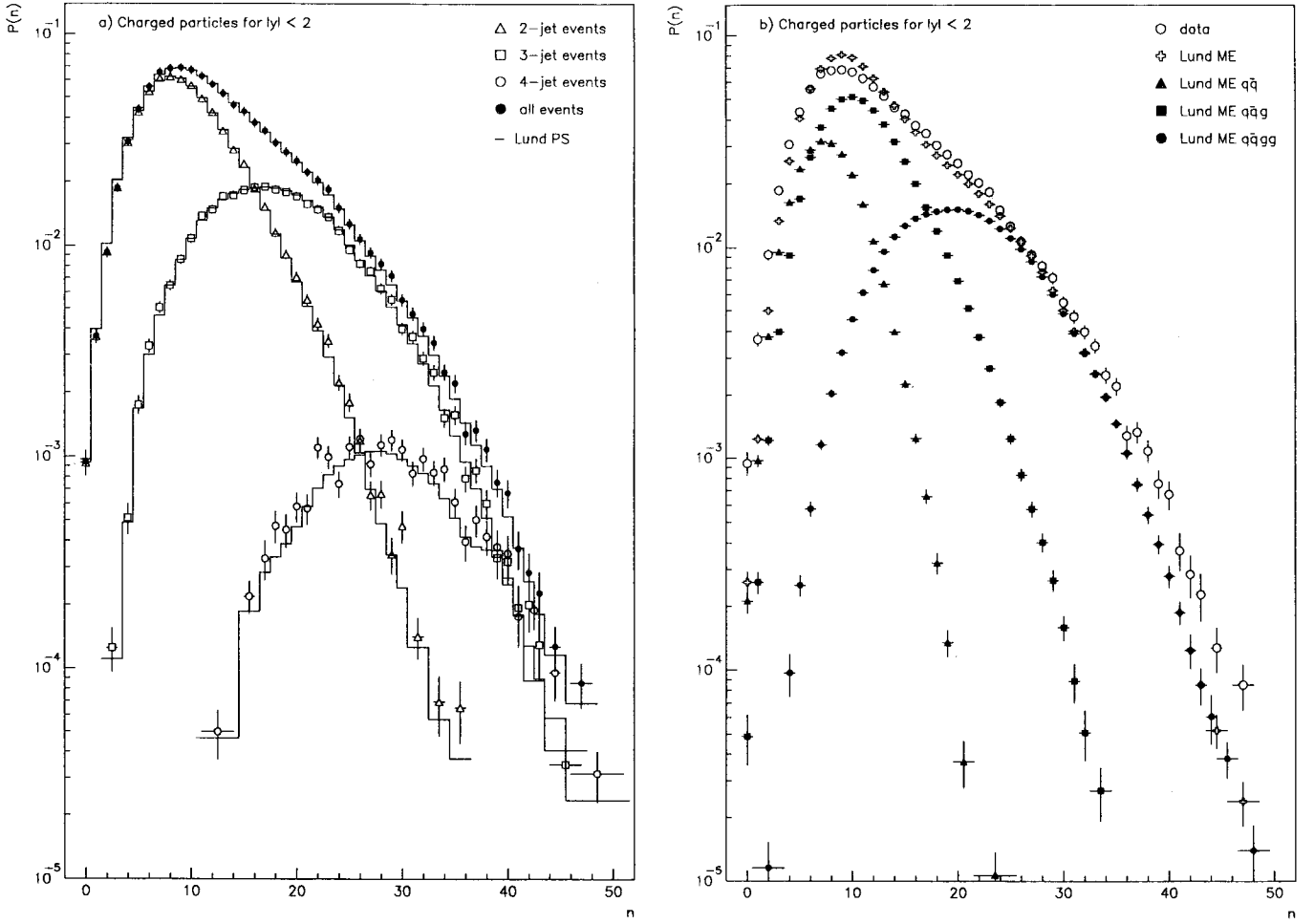
Fig. 3a, b. a Multiplicity distributions $P(n)$ of charged particles for the rapidity range $|y| < 2$ for all events and for events with 2-, 3- and 4-jets, as separated by the JADE jet finding algorithm (for the jet cut resolution $Y_{cut} = 0.04$), in comparison with the Lund PS model predictions; **b** Multiplicity distributions $P(n)$ of charged particles for the rapidity range $|y| < 2$ in comparison with the Lund ME model predictions for the total distributions and for the components due to the $q\bar{q}$, $q\bar{q}g$ and $q\bar{q}gg$ subprocesses

fore fluctuates according to a Poisson distribution with an average $\bar{N}$. The number of particles per clan also fluctuates (on the average according to a logarithmic distribution) with an average $\bar{n}_c$. These two quantities can be derived from the following formulae:

$$\bar{N} = k \cdot \ln(1 + \langle n \rangle / k), \qquad \bar{n}_c = \langle n \rangle / \bar{N},$$

with the parameters $\langle n \rangle$ and $1/k = D^2 / \langle n \rangle^2 - 1/\langle n \rangle$ taken from the experimental data.

The dependence of the average number of clans, $\bar{N}$, on the size of the rapidity interval for our data is compared with the Lund PS model prediction and with the lower energy TASSO data [25] in Fig. 4. The dependence of the average number of particles per clan, $\bar{n}_c$, on the size of the rapidity interval for the same data is presented in Fig. 5. The average number of clans is approximately energy independent in fixed rapidity intervals. On the other hand the average number of charged particles per clan, $\bar{n}_c$, shows strong energy dependence. Thus we observe that a scaling, which fails to hold in particle density [26, 27], holds in clan density. It implies that the multi-

plicity increase with energy is due not to an increased clan density, but to the average clan getting larger in particles and, of course, also due to a wider rapidity range at higher energies. This agrees with conclusions about the "clan picture" made by Giovannini and Van Hove [28] in their "Monte Carlo experiment" based on the Lund PS model* and with the similar results obtained for hadronic collisions [19].

4 Summary and conclusions

The multiplicity distributions in restricted intervals of rapidity have been measured in $e^+ e^-$ collisions at center-of-mass energies close to 91 GeV in the DELPHI experiment at CERN for charged particles emitted in central rapidity intervals and particles emitted in a single hemisphere. The main conclusions are:

---

* The difference in conclusions between our analysis and the one in [28] about the applicability of the NBD can be, most probably, explained by the relatively low statistics of 2000 generated events used in [28]
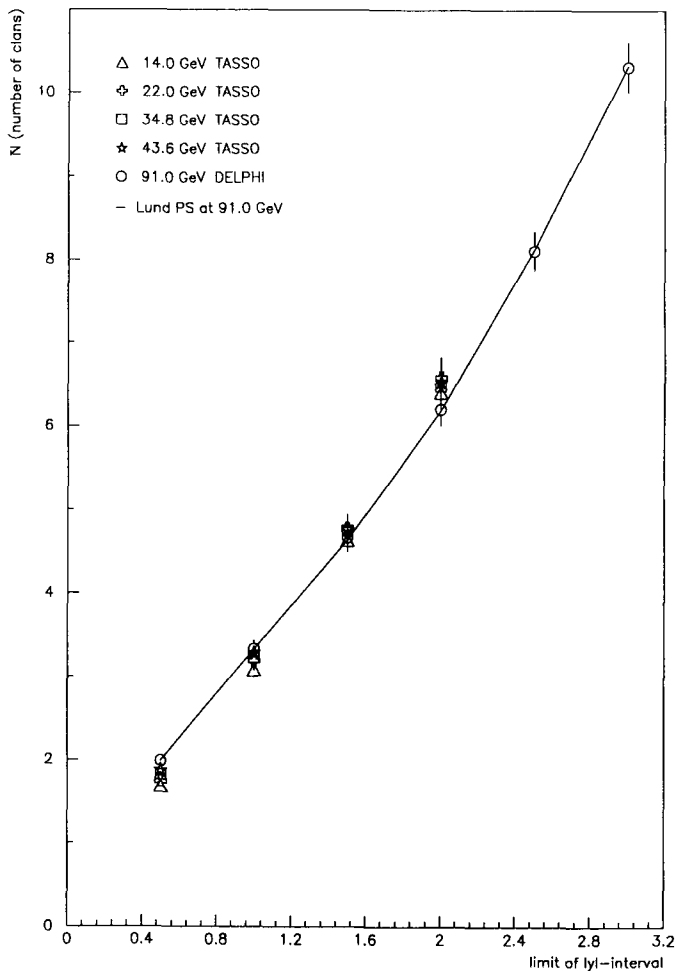
Fig. 4. Average number of clans, $\bar{N}$, for multiplicity distributions of charged particles as a function of the limit of the rapidity interval. Straight lines connect points predicted by the Lund PS model at the center-of-mass energy of 91 GeV. The TASSO data are from [25]
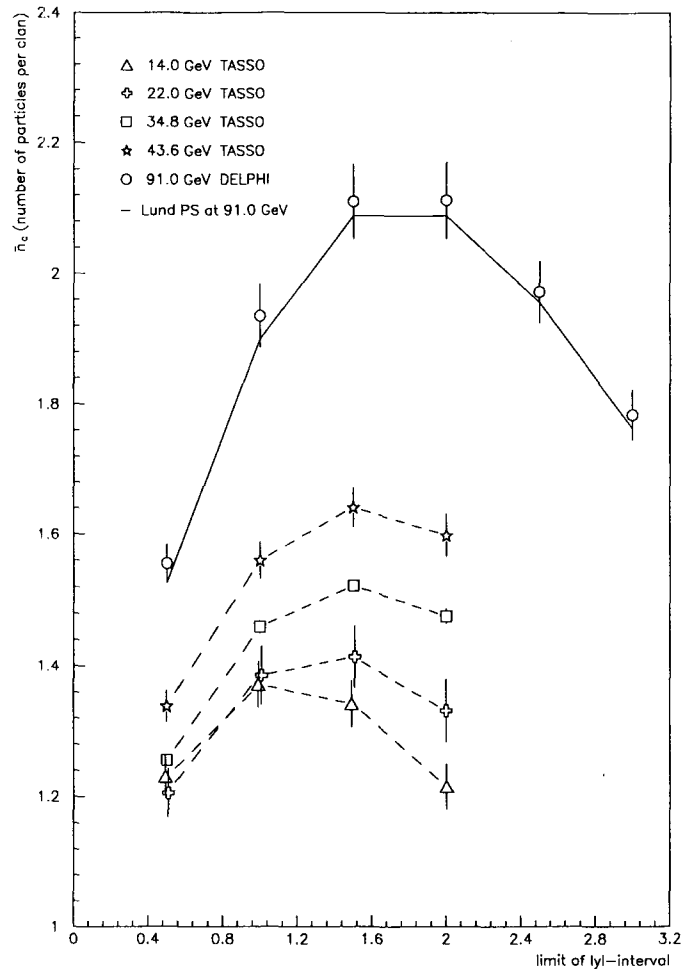
Fig. 5. Average number of charged particles per clan, $\bar{n}_c$, as a function of the limit of the rapidity interval. Straight lines connect points predicted by the Lund PS model at the center-of-mass energy of 91 GeV. The TASSO data points [25] are connected by dashed lines

● The multiplicity distributions in intermediate sized rapidity intervals show a shoulder structure, less evident in full phase space. This structure is explained by the superposition of 2-jet events with mostly low multiplicities and 3- and 4-jet events yielding much larger multiplicities.
● The Lund Parton Shower model describes practically all of the studied features of the multiplicity distributions, including the shoulder structure. The model slightly underestimates the frequency of events in the high multiplicity tails of the distributions, where multi-jet contributions are dominant.
● The negative binomial distributions (NBD) fail to describe the shoulder structure of the multiplicity distributions and thus fail to give good fits to our data. However, the gross shapes, including the high multiplicity tails, are represented by the NBD's. When analysed in terms of independently produced groups of particles, "clans", we find that the average number of clans per event at 91 GeV c.m. energy is approximately the same as at lower energies for each rapidity interval where information ex-

ists, i.e. the clan density with respect to rapidity is approximately energy independent. The multiplicity increase with energy is in this picture due to the average clan containing more particles and also due to the wider rapidity range at higher energies.

References

1. DELPHI Coll., P. Abreu et al.: Z. Phys. C – Particles and Fields 50 (1991) 185
2. M. Bengtsson, T. Sjöstrand: Phys. Lett. B185 (1987) 435
3. T. Sjöstrand: Comput. Phys. Comm. 27 (1982) 243; ibid. 28 (1983) 229; T. Sjöstrand, M. Bengtsson: Comput. Phys. Comm. 43 (1987) 367
4. G. Ekspong: Proc. XVI Intern. Symp. on Multiparticle Dynam-

ics, Kiryat Anavim, 1985, J. Grunhaus (ed.). Editions Frontieres, Singapore: World Scientific 1985, p. 309

5. A. Giovannini, L. Van Hove: Proc. XVII Intern. Symp. on Multiparticle Dynamics Seewinkel, 1986, M. Markytan et al. (eds.). Singapore: World Scientific 1987, p. 561; Z. Phys. C – Particles and Fields 30 (1986) 391

6. L. Van Hove: Physica A147 (1987) 19

7. DELPHI Coll. P. Aarnio et al.: CERN-PPE/90-128 (to appear in NIM) xx

8. Z. Koba, H.B. Nielsen, P. Olesen: Nucl. Phys. B40 (1972) 317

9. JADE Coll. W. Bartel et al.: Z. Phys. C – Particles and Fields 33 (1986) 23; S. Bethke et al.: Phys. Lett. 213B (1988) 235

10. MARK2 Coll. S. Komamiya et al.: Phys. Rev. Lett. 64 (1990) 987

11. OPAL Coll. M.Z. Akrawy et al.: Phys. Lett. 235B (1990) 389

12. DELPHI Coll. P. Abreu et al.: Phys. Lett. 247B (1990) 167

13. W. de Boer, H. Fürstenau, J.H. Köhne: Z. Phys. C – Particles and Fields 49 (1991) 141

14. F. Gutbrod, G. Kramer, G. Schierholz: Z. Phys. C – Particles and Fields 21 (1984) 235; K. Fabricius et al.: Z. Phys. C – Particles and Fields 11 (1981) 315

15. UA5 Coll. R.E. Ansorge et al.: Z. Phys. C – Particles and Fields 43 (1989) 357

16. UA5 Coll. G.J. Alner et al.: Phys. Lett. B160 (1985) 199

17. UA5 Coll. G.J. Alner et al.: Phys. Lett. B160 (1985) 193

18. UA5 Coll. G.J. Alner et al.: Phys. Lett. B167 (1986) 476

19. NA22 Coll. M. Adamus et al.: Z. Phys. C – Particles and Fields 37 (1988) 215; Phys. Lett. B205 (1988) 401

20. EMC Coll. M. Arneodo et al.: Z. Phys. C – Particles and Fields 35 (1987) 335

21. NA5 Coll. F. Dengler et al.: Z. Phys. C – Particles and Fields 33 (1985) 187

22. NA23 Coll. J.L. Bailly et al.: Z. Phys. C – Particles and Fields 40 (1988) 215

23. NA22 Coll. I.V. Ajinenko et al.: Z. Phys. C – Particles and Fields 46 (1990) 569

24. HRS Coll. M. Derrick et al.: Phys. Lett. 168B (1986) 299; Phys. Rev. D34 (1986) 3304

25. TASSO Coll. W. Braunschweig et al.: Z. Phys. C – Particles and Fields 45 (1989) 193

26. ALEPH Coll. D. Decamp et al.: Phys. Lett. 234B (1990) 209

27. DELPHI Coll. P. Abreu et al.: CERN-PPE/90-118 and paper presented to the XXV Int. Conf. on High Energy Physics, Singapore, 1990

28. L. Van Hove, A. Giovannini: Acta Phys. Pol. B19 (1988) 917